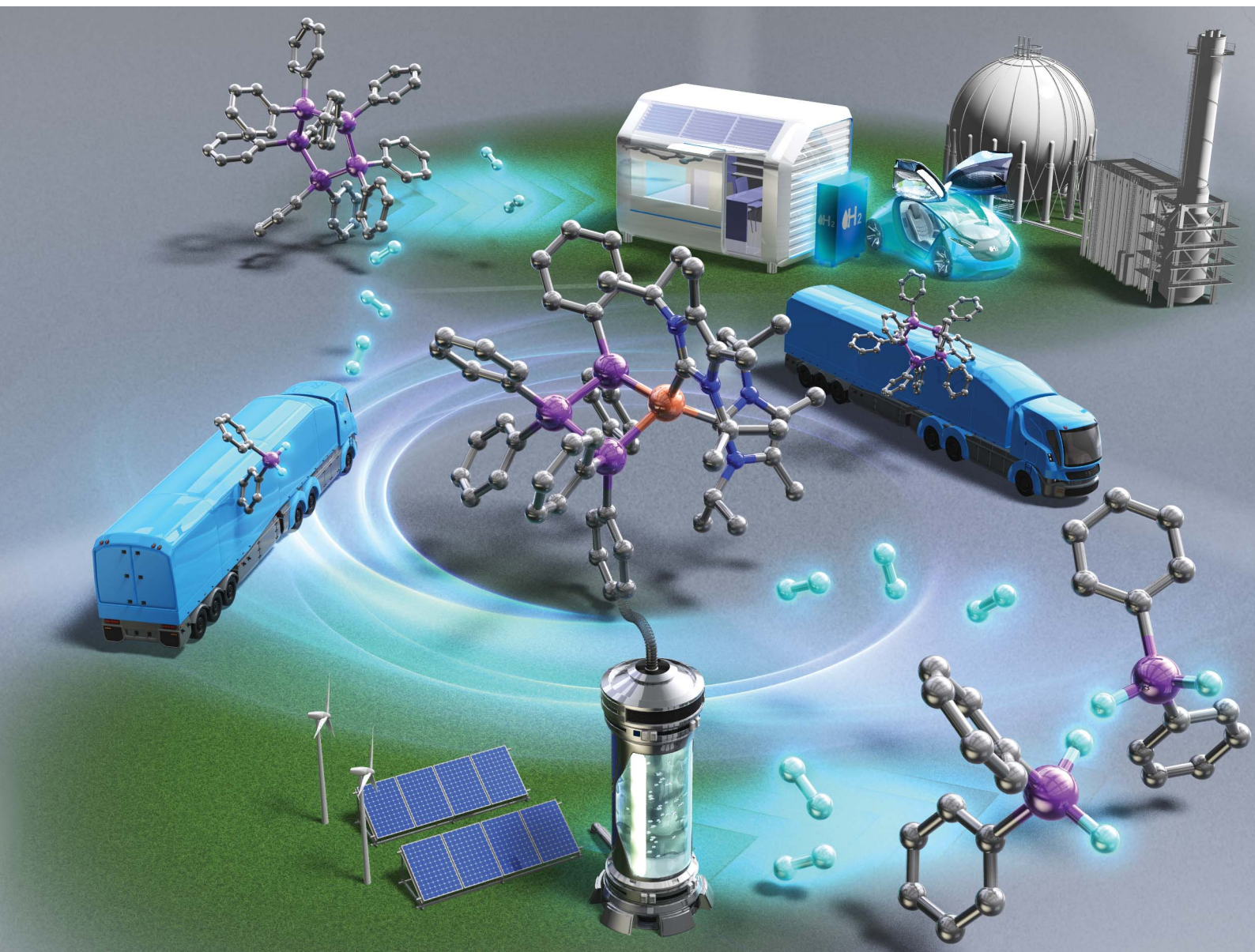


Chemical Science

rsc.li/chemical-science



ISSN 2041-6539

EDGE ARTICLE

Yoshinao Kobayashi and Yusuke Sunada
Germanium hydrides as an efficient hydrogen-storage
material operated by an iron catalyst

Cite this: *Chem. Sci.*, 2023, 14, 1065

All publication charges for this article have been paid for by the Royal Society of Chemistry

Received 31st October 2022
Accepted 29th December 2022

DOI: 10.1039/d2sc06011f

rsc.li/chemical-science

Germanium hydrides as an efficient hydrogen-storage material operated by an iron catalyst†

Yoshinao Kobayashi^a and Yusuke Sunada *^{ab}

The use of metal hydrides such as NaBH₄ as hydrogen-storage materials has recently received substantial research attention on account of the worldwide demand for the development of efficient hydrogen-production, -storage, and -transportation systems. Here, we report the quantitative production of H₂ gas from a germanium hydride, Ph₂GeH₂, mediated by an iron catalyst at room temperature *via* dehydrogenative coupling, concomitant with the formation of (GePh₂)₅. Of particular importance is that Ph₂GeH₂ can be readily recovered from (GePh₂)₅ by contact with 1 atm of H₂ or PhICl₂/LiAlH₄ at 0 °C or 40 °C, respectively. A detailed reaction mechanism for the iron-catalyzed dehydrogenative coupling of Ph₂GeH₂ is proposed based on the isolation of four intermediate iron species.

Introduction

Economic hydrogen production/storage is the key issue preventing the application of hydrogen as an energy carrier in the context of a global low-carbon strategy to address the ever-increasing energy challenges that face humanity. Recently, a number of hydrogen storage materials, such as metal hydrides, liquid organic hydrogen carriers, ammonia and ammonia borane, were applied for the development of effective hydrogen production/storage systems.¹ Among them, metal hydrides have attracted great attention recently as potential efficient hydrogen-storage materials. Sodium borohydride (NaBH₄) is one of the most studied hydrides for this purpose, as it is able to deliver H₂ gas under mild conditions, *e.g.*, at room temperature, *via* hydrolysis.² However, one major issue with this approach is that the regeneration of NaBH₄ from the hydrolytic products formed after H₂ production generally carries a high energy penalty and thus requires, *e.g.*, high temperatures (400–500 °C). Thus, the development of hydrogen-production/-storage systems in which the generation of H₂ can proceed under mild conditions and hydrogen-storage materials that can be regenerated easily is highly desirable.

In this paper, we focus on the use of group-14 hydrides as potentially reusable hydrogen-storage materials. It is well known that group-14 hydrides such as hydrosilanes, hydrogermanes, and hydrostannanes undergo dehydrogenative coupling reactions in the presence of appropriate transition-

metal catalysts to form E–E (E = Si, Ge, Sn) bond(s), concomitant with the generation of H₂.³ A pioneering study in this area has been published by Harrod and co-workers, who reported that hydrosilanes such as PhSiH₃ effectively undergo multiple Si–Si-bond-forming reactions in a dehydrogenative manner to afford polysilanes and/or a mixture of oligosilanes.⁴ This study revealed that hydrosilanes can act as reagents for hydrogen-production and E–E-bond-formation reactions; however, the regeneration of the starting hydrosilanes is considered to be challenging because high-molecular-weight polymeric compounds are obtained as the major products after the production of H₂. Although polymeric products have mainly been obtained in catalyst systems based on early transition metals,⁵ it has been reported that late-transition-metal catalysts often tend to afford relatively short-chain oligomers in the dehydrogenative coupling of group-14 hydrides.⁶ For instance, Rosenberg *et al.* have indicated that the dehydrogenative coupling of Ph₂SiH₂ catalyzed by Rh(PPh₃)₃Cl affords the disilane Ph₂(H)Si–Si(H)Ph₂ selectively under the optimal reaction conditions;^{5b} however, no attempts to regenerate Ph₂SiH₂ from Ph₂(H)Si–Si(H)Ph₂ have been reported in the same study. Although some examples of the reverse reaction of the dehydrogenative coupling of hydrosilanes, *i.e.*, hydrogenolysis of disilanes to afford hydrosilanes, have been reported for Ni or Pt catalysts,⁷ reversible and reusable hydrogen-production/-storage systems with group-14 hydrides have not been explored so far.

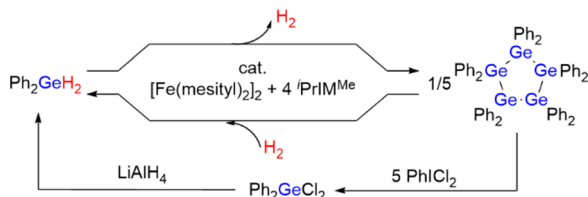
In this work, we developed a catalytic system based on iron for the reversible production/storage of H₂ using germanium hydrides as the potential hydrogen-storage material because iron is the least expensive and least toxic late transition metal (Scheme 1). We found that the combination of the iron precursor [Fe(mesityl)₂]₂ (mesityl = 2,4,6-Me₃-C₆H₂) with *N*-heterocyclic carbene (NHC) ligands promotes the effective

^aDepartment of Applied Chemistry, School of Engineering, The University of Tokyo, 4-6-1, Komaba, Meguro-ku, Tokyo 153-8505, Japan

^bInstitute of Industrial Science, The University of Tokyo, 4-6-1, Komaba, Meguro-ku, Tokyo 153-8505, Japan. E-mail: sunada@iis.u-tokyo.ac.jp

† Electronic supplementary information (ESI) available. CCDC 2204746, 2204747, 2204748 and 2204749. For ESI and crystallographic data in CIF or other electronic format see DOI: <https://doi.org/10.1039/d2sc06011f>





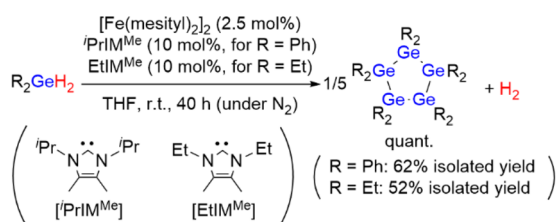
Scheme 1 Overall scheme of this work; Ph_2GeH_2 as a reusable hydrogen-storage material in the presence of an iron catalyst.

production of H_2 in the dehydrogenative coupling of R_2GeH_2 ($\text{R} = \text{Ph}$ or Et) (hydrogen content: *ca.* 0.87 wt% for Ph_2GeH_2 and *ca.* 1.51 wt% for Et_2GeH_2). The quantitative generation of H_2 at room temperature using Ph_2GeH_2 as a hydrogen-storage material was confirmed, along with the formation of $(\text{GePh}_2)_5$ as the dehydrogenative coupling product. It is noteworthy that the starting Ph_2GeH_2 can be readily regenerated *via* the hydrogenation of $(\text{GePh}_2)_5$ under 1 atm of H_2 at 0°C catalyzed by the same iron catalyst system. Alternatively, Ph_2GeH_2 can also be recovered from $(\text{GePh}_2)_5$ by treatment with PhICl_2 followed by LiAlH_4 at 40°C . These results show the promising potential of germanium hydrides as prospective reusable hydrogen-production/-storage materials that can evolve H_2 at room temperature using an iron catalyst. Moreover, four possible intermediary iron species formed in this catalysis were structurally characterized, based on which, a detailed reaction mechanism is proposed. The present catalyst system is also applicable to the dehydrogenative coupling of other group-14 hydrides, such as hydrosilanes and hydrostannanes R_2EH_2 ($\text{E} = \text{Si}, \text{Sn}$).

Results and discussion

Hydrogen production from secondary germanes

First, the diphenylgermane Ph_2GeH_2 was used as the substrate, and the dinuclear iron(II) complex $[\text{Fe}(\text{mesityl})_2]_2$ (mesityl = 2,4,6-trimethylphenyl) was used as the catalyst precursor, because it has been reported to effectively activate group-14-element-hydrogen bonds.⁸ The dehydrogenative coupling of Ph_2GeH_2 proceeded effectively at room temperature in THF under an N_2 atmosphere when a mixture of 2.5 mol% of $[\text{Fe}(\text{mesityl})_2]_2$ (5 mol% based on Fe) and 10 mol% of the *N*-heterocyclic carbene ${}^i\text{PrIMe}$ (${}^i\text{PrIMe} = 1,3$ -diisopropyl-4,5-dimethylimidazol-2-ylidene) was used as the catalyst (Scheme



Scheme 2 Catalytic dehydrogenative coupling of Ph_2GeH_2 or Et_2GeH_2 catalyzed by the $[\text{Fe}(\text{mesityl})_2]_2/\text{NHC}$ catalyst system.

2). This reaction furnished cyclic pentagermane $(\text{GePh}_2)_5$ as the sole product in 62% isolated yield after 40 h. The formation of $(\text{GePh}_2)_5$ was confirmed based on a comparison of the ${}^1\text{H}$ and ${}^{13}\text{C}$ NMR spectra of the product with those of an authentic sample.⁹ It is noteworthy that the formation of $(\text{GePh}_2)_5$ was accompanied by the generation of H_2 gas, which was confirmed by ${}^1\text{H}$ NMR spectroscopy. The quantity of H_2 gas produced was determined using a gas burette; when the dehydrogenative coupling of 1 mmol of Ph_2GeH_2 was performed at room temperature under the catalytic conditions described above, *ca.* 21 mL of gaseous product(s) were obtained in the gas burette. These results indicate that the dehydrogenation of Ph_2GeH_2 to afford $(\text{GePh}_2)_5$ proceeded effectively at room temperature to give a quantitative amount of H_2 gas.

It should be emphasized here that this catalysis is highly sensitive to the electronic and/or steric environment of the ligands used. Thus, ${}^i\text{PrIMe}$ was found to be the only ligand that selectively furnished $(\text{GePh}_2)_5$ for a quantitative conversion of Ph_2GeH_2 , and that other NHC ligands used in this study with different substituents on the nitrogen atoms or the ligand backbone barely generated any $(\text{GePh}_2)_5$. Although the use of certain NHC ligands led to a high conversion of Ph_2GeH_2 , the formation of a mixture of oligogermanes other than $(\text{GePh}_2)_5$ was suggested by the ${}^1\text{H}$ NMR spectra of the corresponding crude products (for details, see Table S2 in the ESI†). Subsequently, we examined the effect of the solvent on the reaction of Ph_2GeH_2 catalyzed by $[\text{Fe}(\text{mesityl})_2]_2/{}^i\text{PrIMe}$, which revealed that the use of ethereal solvents such as Et_2O and THF afforded $(\text{GePh}_2)_5$ in medium to good yield.

Subsequently, the dehydrogenative coupling of Et_2GeH_2 was performed using $[\text{Fe}(\text{mesityl})_2]_2/{}^i\text{PrIMe}$. Although the conversion of Et_2GeH_2 reached >99% in THF after 40 h, the ${}^1\text{H}$ NMR spectrum of the crude product suggested the formation of a complex mixture of oligogermanes, and almost no formation of cyclopentagermane $(\text{GeEt}_2)_5$ was observed. This result stands in stark contrast to the fact that the selective production of $(\text{GeEt}_2)_5$ with >99% conversion (52% isolated yield) of Et_2GeH_2 was confirmed when EtIMe was used instead of ${}^i\text{PrIMe}$ (Scheme 2). These results indicate that sophisticated control of the steric environment around the iron center on the catalytically active species can be expected to be crucial to achieving the dehydrogenative coupling of secondary germanes in a selective manner to produce the corresponding cyclopentagermanes $(\text{GeR}_2)_5$ ($\text{R} = \text{Ph}, \text{Et}$) as a single product. It should also be noted here that although cyclooligogermanes are usually generated *via* the Wurtz-type reductive coupling of R_2GeX_2 ($\text{R} = \text{alkyl}, \text{aryl}$; $\text{X} = \text{halide}$) using a stoichiometric amount of alkali or alkaline earth metals,¹⁰ the development of alternative synthetic methods would be highly desirable due to the harsh reaction conditions required. The dehydrogenative coupling of secondary germanes could be a potential alternative to such Wurtz-type reductive coupling reactions in terms of the formation of Ge-Ge bonds, although previously reported examples of the catalytic dehydrogenative coupling of secondary germanes only furnished dimers. To the best of our knowledge, the results shown here thus represent the first example of the formation of cyclooligogermanes *via* the sequential catalytic dehydrogenative



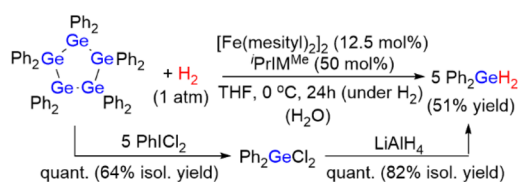
coupling of secondary germanes under the formation of multiple Ge–Ge bonds.

Regeneration of Ph_2GeH_2 from $(\text{GePh}_2)_5$

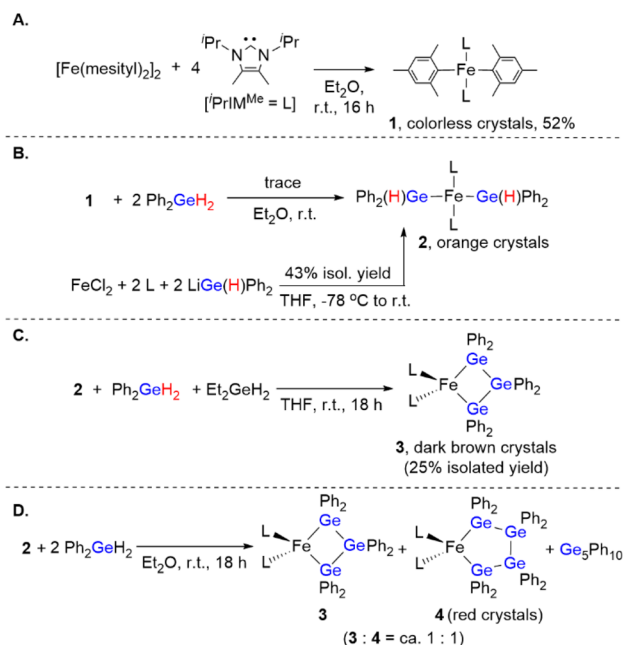
We discovered that the starting material Ph_2GeH_2 can be readily regenerated from $(\text{GePh}_2)_5$ by treatment with 1 atom of H_2 in the presence of $[\text{Fe}(\text{mesityl})_2]_2/{}^i\text{PrIM}^{\text{Me}}$ in THF at 0°C for 24 h, *i.e.*, Ph_2GeH_2 was formed in 51% yield. It was also confirmed that no reaction occurred when $(\text{GePh}_2)_5$ was exposed to 1 atm of H_2 in the absence of an iron catalyst. The regeneration of Ph_2GeH_2 was accompanied by the formation of germoxane $(\text{Ph}_2\text{GeO})_3$ in 49% yield; this is presumably due to the rapid hydrolysis of the formed Ph_2GeH_2 induced by ${}^i\text{PrIM}^{\text{Me}}$ and unremovable traces of H_2O . It should also be noted here that hydrosilanes such as Ph_2SiH_2 undergo fast hydrolysis in the presence of a catalytic amount of *N*-heterocyclic carbenes.¹¹ Although the quantitative formation of Ph_2GeH_2 from $(\text{GePh}_2)_5$ and H_2 gas was hampered despite many attempts to remove the aforementioned trace amounts of H_2O , we found that Ph_2GeH_2 could be readily recovered from $(\text{GePh}_2)_5$ *via* an alternative method; $(\text{GePh}_2)_5$ can be converted quantitatively into Ph_2GeCl_2 (64% isolated yield) by treatment with PhICl_2 in THF at 40°C , before Ph_2GeCl_2 can be quantitatively transformed into Ph_2GeH_2 by reaction with LiAlH_4 in THF at room temperature (82% isolated yield) (Scheme 3). Thus, we concluded that the germanium hydride Ph_2GeH_2 was easily recovered and reused *via* two independent reaction protocols. These results corroborate the notion that Ph_2GeH_2 is an effective and reusable hydrogen-storage material that can quantitatively produce H_2 gas at mild operating temperatures and that can be readily regenerated from $(\text{GePh}_2)_5$ through hydrogenation under 1 atm of H_2 gas or sequential treatment with PhICl_2 and LiAlH_4 .

Isolation of four possible intermediary iron species

To obtain insight into the reaction mechanism of the $[\text{Fe}(\text{mesityl})_2]_2/{}^i\text{PrIM}^{\text{Me}}$ -catalyzed dehydrogenative coupling of Ph_2GeH_2 to produce $(\text{GePh}_2)_5$, several investigations were carried out to isolate any potential intermediary iron species. Initially, the reaction of $[\text{Fe}(\text{mesityl})_2]_2$ and 4 equivalents of ${}^i\text{PrIM}^{\text{Me}}$ was carried out in Et_2O at room temperature for 16 h, which provided mononuclear *trans*- $\text{Fe}(\text{mesityl})_2({}^i\text{PrIM}^{\text{Me}})_2$ (**1**) in 52% isolated yield (Scheme 4A). A single-crystal X-ray diffraction (XRD) analysis revealed that the iron center in **1** adopts a square-planar geometry with two ${}^i\text{PrIM}^{\text{Me}}$ ligands located at the *trans*-positions, which is similar to that observed in a previously reported analogous $\text{Fe}(\text{mesityl})_2({}^i\text{PmIM}^{\text{H}})_2$ complex.^{8b} Subsequently, isolated complex **1** was treated with 2



Scheme 3 Regeneration of Ph_2GeH_2 from $(\text{GePh}_2)_5$.



Scheme 4 Synthesis of iron complexes **1**–**4**. (A) Synthesis and isolation of **1**. (B) Two reaction schemes for the synthesis of **2**. (C) Synthesis and isolation of **3**. (D) Synthesis of *ca.* a 1 : 1 mixture of iron complexes **3** and **4**.

equivalents of Ph_2GeH_2 , which produced a trace amount of orange crystals of *trans*- $\text{Fe}(\text{GePh}_2\text{H}_2)_2({}^i\text{PrIM}^{\text{Me}})_2$ (**2**), together with a white powder of $(\text{GePh}_2)_5$. Although the isolation of pure **2** from this reaction was hampered by the concomitant formation of $(\text{GePh}_2)_5$, **2** was isolated using an alternative reaction protocol. Namely, the reaction of FeCl_2 with *in situ*-generated $\text{LiGe}(\text{H})\text{Ph}_2$ in the presence of 2 equivalents of ${}^i\text{PrIM}^{\text{Me}}$ in THF led to the isolation of **2** in 43% yield (Scheme 4B). The molecular structure of **2** was determined by single-crystal XRD analysis (Fig. 1A). Similar to that in complex **1**, the iron center in **2** adopts a square-planar coordination geometry wherein two ${}^i\text{PrIM}^{\text{Me}}$ ligands occupy *trans*-positions. To the best of our knowledge, complex **2** is the first example of an $\text{Fe}(\text{II})$ -germyl complex with a four-coordinate square-planar coordination geometry. The Fe–Ge bond distances of 2.4488(8) Å are longer than those in previously reported iron(II) germyl complexes with octahedral structures ($\text{Cp}^*\text{Fe}(\text{CO})_2(\text{GeMe}_2\text{SPh})$: 2.3633(4) Å;¹² $\text{CpFe}(\text{CO})(\text{pyridine})(\text{GeEt}_3)$: 2.4055(11) Å;¹³ $\text{Cp}(\text{CO})_2[\text{Ge}(\text{C}_2\text{F}_5)_3]$: for 2.3232(3) Å;¹⁴). This is presumably due to the strong *trans*-influence of the germyl moieties. In the IR spectrum of **2**, an absorption band observed at 1848 cm^{-1} implied the presence of Ge–H bonds in **2**.

Based on the molecular structure of **2**, the first H–Ge bond activation mediated by **1** can be assumed to take place through the Fe-mesityl moiety. A similar reaction, *i.e.*, the formation of square-planar *trans*- $(\text{NHC})_2\text{Fe}(\text{Sn}^n\text{Bu}_3)_2$ *via* the reaction of *trans*- $(\text{NHC})\text{Fe}(\text{mesityl})_2$ with ${}^n\text{Bu}_3\text{SnH}$, has recently been reported by Radius *et al.*^{8b} Further treatment of **2** with 1 equivalent of Ph_2GeH_2 and 1 equivalent of Et_2GeH_2 led to the formation of a Ge–Ge bond on the iron center to afford complex **3**, which



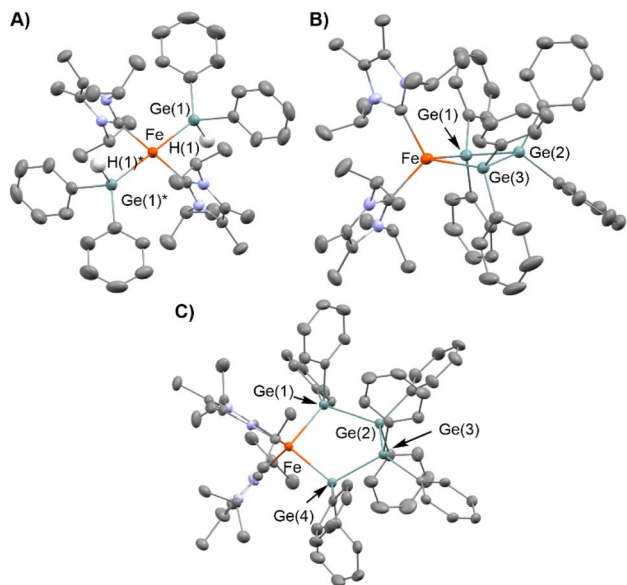


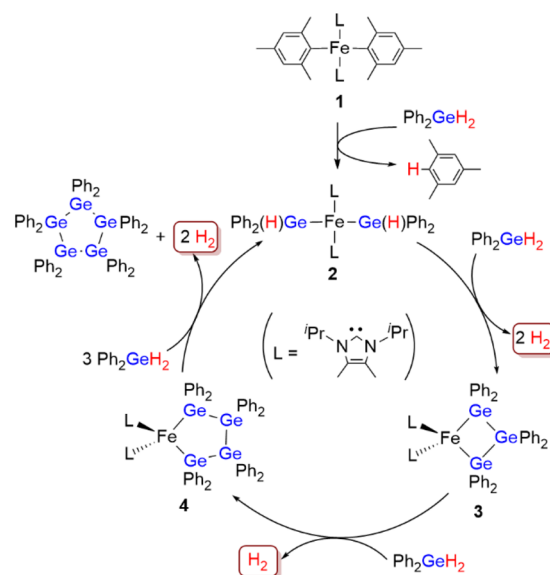
Fig. 1 Molecular structures of **2**, **3** and **4** with thermal ellipsoids at 50% probability; hydrogen atoms, except for the hydrides in **2**, have been omitted for clarity. (A) Molecular structure of **2**. (B) Molecular structure of **3**. (C) Molecular structure of **4**.

contains a metallatrigermacycle skeleton, in 25% isolated yield (Scheme 4C). Although the actual role of Et_2GeH_2 in this reaction remains unclear so far, Et_2GeH_2 may contribute to retarding the rate of the reaction between **2** and Ph_2GeH_2 , thus leading to the production of complex **3** as the main product. The molecular structure of **3** (Fig. 1B) revealed that the iron center adopts a tetrahedral coordination geometry, which is different from those found in **1** and **2**. The Fe–Ge bond distances in **3** (2.5712(6)/2.5557(5) Å) are elongated compared to those in **2** and other previously reported iron(II) germyl complexes,^{12–14} although they are comparable to that of our previously reported iron(II) digermyl complex with a tetrahedral coordination geometry, $(\text{THF})_2\text{Fe}[\text{Ge}(\text{SiMe}_3)_3]_2$ (2.5589(8) Å).¹⁵ The iron center and three germanium atoms form a nearly planar metallacyclic skeleton, wherein the deviation of all atoms from the least-squares plane ranges from 0.116 Å to 0.124 Å. It is worth noting here that the Ge–Ge-bond-forming reaction apparently occurs during the reaction of **2** with Ph_2GeH_2 to produce **3**. In other words, the bond formation involving two Fe–Ge bonds and an incoming molecule of Ph_2GeH_2 to construct a cyclic trigermyl moiety is effectively promoted on the iron center supported by $^i\text{PrIM}^{\text{Me}}$ ligands. The ^1H NMR spectrum of isolated **3** in C_6D_6 at room temperature features broad resonances at $\delta = 27.2$, 21.3, 19.8, 15.8, 14.3, 7.5, and -1.2 ppm, indicating that **3** is paramagnetic.

We found that a new iron species **4** is formed together with **3** and $(\text{GePh}_2)_5$ in the reaction between **2** and 2 equivalents of Ph_2GeH_2 (Scheme 4D). Although several attempts to isolate **4** failed, a subsequent recrystallization led to the generation of reddish crystals, whose ^1H NMR spectrum in C_6D_6 indicated that they consist of a *ca.* 1 : 1 mixture of **3** and **4**. A careful single-crystal XRD analysis revealed the molecular structure of **4**,

which consists of a five-membered metallatetragermacycle skeleton composed of four ‘ GePh_2 ’ moieties (Fig. 1C). The iron center of **4** adopts a slightly distorted tetrahedral coordination geometry with Fe–Ge bond lengths of 2.5714(10) and 2.5840(9) Å. These structural features are similar to those in **3**; however, there are apparent, significant differences in the metallacycle framework. Namely, the four-membered-ring structure in **3** is almost planar, whereas that of **4** exhibits a $^{\text{Ge}(2)}\text{T}_{\text{Ge}(3)}$ -type twisted structure.¹⁶ The average Ge–Ge bond length (~ 2.459 Å) in **4** is also comparable to that in **3** (~ 2.477 Å). Based on the molecular structure of **4**, one might consider that the incorporation of one additional ‘ GePh_2 ’ unit into **3** led to the generation of **4** *via* Ge–Ge bond propagation.

With the four possible intermediary iron species **1–4** in hand, we would like to propose a reaction mechanism for the dehydrogenative coupling of Ph_2GeH_2 catalyzed by the $[\text{Fe}(\text{mesityl})_2]_2/{}^i\text{PrIM}^{\text{Me}}$ catalyst system as shown in Scheme 5. First, $[\text{Fe}(\text{mesityl})_2]_2$ reacts with ${}^i\text{PrIM}^{\text{Me}}$ to generate catalyst precursor **1**. Then, Ge–H bond activation of two moles of Ph_2GeH_2 occurs *via* the Fe–mesityl bonds in **1** to generate the catalytically active species **2**. A sequence of Ge–Ge-bond-forming and Ge–Ge-bond-propagation reactions occurs on the iron center supported by the two ${}^i\text{PrIM}^{\text{Me}}$ ligands to generate **3** followed by **4**, both of which feature metallacyclopolygermane frameworks. Finally, the incorporation of an additional ‘ GePh_2 ’ unit proceeds when **4** comes into contact with Ph_2GeH_2 to produce $(\text{GePh}_2)_5$ with concomitant regeneration of **2**. In summary, ‘ GePh_2 ’ units sequentially assemble on the iron center to realize the selective production of $(\text{GePh}_2)_5$ *via* dehydrogenative coupling. It should be noted here that the catalytic activity of the isolated complexes **1**, **2** and **3** was examined independently and that both showed good catalytic activity



Scheme 5 Plausible reaction mechanism for the sequential production of H_2 and Ge–Ge bond propagation to afford cyclopentagermane $(\text{GePh}_2)_5$ *via* the dehydrogenative coupling of Ph_2GeH_2 catalyzed by $[\text{Fe}(\text{mesityl})_2]_2/{}^i\text{PrIM}^{\text{Me}}$.

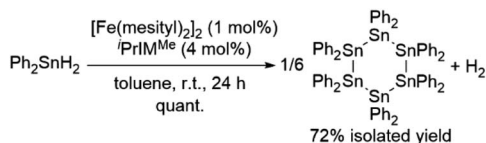


toward the dehydrogenative coupling of Ph_2GeH_2 to afford $(\text{GePh}_2)_5$ in quantitative yield in THF at room temperature after 40 h (5 mol% of **1**, **2** or **3**). This result strongly supports the notion that the iron species **2** and **3** play a crucial role in the catalytic dehydrogenative coupling of Ph_2GeH_2 .

Dehydrogenative coupling of other group-14 hydrides

As described above, the $[\text{Fe}(\text{mesityl})_2]_2/\text{NHC}$ catalyst system is effective for H_2 production *via* the dehydrogenative coupling of secondary germanes. We found that the dehydrogenative coupling of tertiary and primary germanes can also be achieved by this catalyst system. For instance, the dehydrogenative coupling of Ph_3GeH proceeded effectively in THF at room temperature mediated by 2.5 mol% of $[\text{Fe}(\text{mesityl})_2]_2$ in the presence of 10 mol% of MeIM^{Et} , which contains sterically less demanding methyl groups on the nitrogen atoms of the NHC ligand, to selectively afford the dimeric product $(\text{GePh}_3)_2$. Similarly, the reaction with $t\text{BuGeH}_3$ was briefly examined, and the formation of oligogermanes *via* the dehydrogenative coupling mediated by a catalytic amount of $[\text{Fe}(\text{mesityl})_2]_2/{}^i\text{PrIM}^{\text{Me}}$ was observed using ${}^1\text{H}$ NMR and FAB-MS.

Tin hydrides such as Ph_2SnH_2 and ${}^n\text{Bu}_2\text{SnH}_2$ were also found to be suitable for this catalytic system (hydrogen content: *ca.* 0.73 wt% for Ph_2SnH_2 and *ca.* 0.85 wt% for ${}^n\text{Bu}_2\text{SnH}_2$). Namely, 1 mmol of Ph_2SnH_2 was dehydrogenatively coupled in the presence of 1 mol% of $[\text{Fe}(\text{mesityl})_2]_2$ and 4 mol% of ${}^i\text{PrIM}^{\text{Me}}$ to exclusively produce cyclohexastannane $(\text{SnPh}_2)_6$, which was isolated in 70% yield. The quantity of H_2 gas produced in the course of this reaction was determined using a gas burette, from which *ca.* 15.4 mL of gaseous product(s) were obtained after 2.5 h at room temperature, and then production of *ca.* 16.7 mL of gaseous product(s) was detected after 19 h. In this reaction, the production of H_2 immediately took place once Ph_2SnH_2 came into contact with $[\text{Fe}(\text{mesityl})_2]_2/{}^i\text{PrIM}^{\text{Me}}$, and this may cause decrease of the amount of detectable gaseous H_2 compared with the theoretical value (*ca.* 22 mL). In contrast to the reaction with germanium congener Ph_2GeH_2 , the reaction with Ph_2SnH_2 exclusively afforded cyclohexastannane. ${}^n\text{Bu}_2\text{SnH}_2$ was also found to be suitable for this catalyst system (1 mol% of $[\text{Fe}(\text{mesityl})_2]_2$ and 4 mol% of ${}^i\text{PrIM}^{\text{Me}}$) to give a *ca.* 3:1 mixture of cyclopentastannane $(\text{Sn}^n\text{Bu}_2)_5$ and cyclohexastannane $(\text{Sn}^n\text{Bu}_2)_6$ with complete conversion of ${}^n\text{Bu}_2\text{SnH}_2$ at room temperature (Scheme 6). In this context, it should also be noted that the formation of a mixture of $(\text{Sn}^n\text{Bu}_2)_5$ and $(\text{Sn}^n\text{Bu}_2)_6$ has already been reported by Jousseume *et al.* in the $(\text{PPh}_3)_2\text{PdCl}_2$ -catalyzed dehydrogenative coupling of ${}^n\text{Bu}_2\text{SnH}_2$.¹⁷



Scheme 6 Catalytic dehydrogenative coupling of Ph_2SnH_2 catalyzed by the $[\text{Fe}(\text{mesityl})_2]_2/\text{NHC}$ catalyst system.

The iron-based catalyst system described here was found to be effective under mild reaction conditions for the dehydrogenative coupling of primary, secondary, and tertiary germanes as well as secondary stannanes. Although a relatively high reaction temperature was required, the dehydrogenative coupling of a secondary silane was also achieved by an $[\text{Fe}(\text{mesityl})_2]_2/{}^i\text{PrIM}^{\text{Me}}$ catalyst system. Neat Ph_2SiH_2 (hydrogen content: *ca.* 1.01 wt%) was treated with 2.5 mol% of $[\text{Fe}(\text{mesityl})_2]_2$ and 10 mol% of ${}^i\text{PrIM}^{\text{Me}}$ at 80 °C. The ${}^1\text{H}$ NMR spectrum of the crude product indicated 82% conversion of Ph_2SiH_2 and the generation of the disilane $\text{Ph}_2(\text{H})\text{Si}-\text{Si}(\text{H})\text{Ph}_2$ and trisilane $\text{Ph}_2(\text{H})\text{Si}-\text{SiPh}_2-\text{Si}(\text{H})\text{Ph}_2$ in 54% and 8% yield, respectively. In contrast to the reaction systems with secondary germanes and stannanes, no further propagation of the 'SiPh₂' units took place in this reaction; instead, the generation of Ph_3SiH and PhSiH_3 was detected due to concomitant redistribution. It should be mentioned here that Rosenberg *et al.* have already reported the selective formation of $\text{Ph}_2(\text{H})\text{Si}-\text{Si}(\text{H})\text{Ph}_2$ *via* the dehydrogenative coupling of Ph_2SiH_2 catalyzed by $\text{Rh}(\text{PPh}_3)_3\text{Cl}$. In their report, the authors mentioned that the chemoselectivity of this reaction strongly depends on the reaction conditions, including the size of the reaction vial relative to the volume of the substrate, as well as the rate and efficacy of stirring, and that trisilanes and other redistribution products are often generated under non-optimized reaction conditions. This precedent might suggest that the chemoselectivity of our reaction with Ph_2SiH_2 could be improved by the optimization of the reaction conditions. However, unfortunately, neither the conversion of Ph_2SiH_2 nor the chemoselectivity were improved under either different reaction conditions or the use of catalyst systems that contained different auxiliary ligands.

Conclusions

Germanium hydride Ph_2GeH_2 can act as an efficient and reusable hydrogen-production/-storage material with the aid of iron catalysts. Hydrogen evolution from Ph_2GeH_2 was effectively realized at room temperature, concomitant with the quantitative formation of $(\text{GePh}_2)_5$. The regeneration of Ph_2GeH_2 is very facile, *i.e.*, by simple treatment of $(\text{GePh}_2)_5$ with 1 atm of H_2 at 0 °C, or by treatment with PhICl_2 and LiAlH_4 at 40 °C. This hydrogen-production/-storage system has some advantages compared to systems based on conventional hydrogen-storage materials such as NaBH_4 , in which both the hydrogen-production and -storage processes can be carried out under relatively mild operating conditions, and that they do not require precious-metal catalysts. Furthermore, germanium hydrides are generally sufficiently stable under aerobic conditions, easy-to-handle, and show less toxicity toward living organisms. We expect that the results presented in this paper will help in developing the next generation of chemical hydrogen-storage/-production systems and support efforts to use group-14 hydrides such as germanium hydrides as reusable hydrogen carriers in practical applications, which are currently in progress in our laboratory.



Data availability

All experimental data are provided in the ESI.†

Author contributions

Y. Kobayashi conducted all experiments. All authors analysed the data. Y. Sunada supervised this study and wrote the manuscript. All authors discussed the results and contributed to the preparation of the final manuscript.

Conflicts of interest

There are no conflicts to declare.

Acknowledgements

This work was supported by a project of the Kanagawa Institute of Industrial Science and Technology (KISTEC) as well as by a Grant in Aid for Scientific Research (B) (20H02751) from the Ministry of Education, Culture, Sports, Science and Technology (MEXT), Japan. The synchrotron radiation experiments were performed at the BL02B1 of SPring-8 with the approval of the Japan Synchrotron Radiation Research Institute (JASRI) (Proposal No. 2021A1139).

Notes and references

- (a) M. D. Allendorf, V. Stavila, J. L. Snider, M. Witman, M. E. Bowden, K. Brooks and T. Autrey, *Nat. Chem.*, 2022, **14**, 1214–1223; (b) T. He, P. Pachfule, H. Wu, Q. Xu and P. Chen, *Nat. Rev. Mater.*, 2016, **1**, 1–17; (c) M. R. Usman, *Renew. Sustain. Energy Rev.*, 2022, **167**, 112743; (d) A. Kovač, M. Paranos and D. Marciuš, *Int. J. Hydrog. Energy*, 2021, **46**, 10016–10035; (e) T. He, H. Cao and P. Chen, *Adv. Mater.*, 2019, **31**, 1902757; (f) A. Schneemann, J. L. White, S. Kang, S. Jeong, L. F. Wan, E. S. Cho and V. Stavila, *Chem. Rev.*, 2018, **118**, 10775–10839; (g) M. Paskevicius, L. H. Jepsen, P. Schouwink, R. Černý, D. B. Ravnsbæk, Y. Filinchuk and T. R. Jensen, *Chem. Soc. Rev.*, 2017, **46**, 1565–1634; (h) P. Jena, *J. Phys. Chem. Lett.*, 2011, **2**, 206–211; (i) J. Yang, A. Sudik, C. Wolverton and D. J. Siegel, *Chem. Soc. Rev.*, 2010, **39**, 656–675.
- (a) H. I. Schlesinger, H. C. Brown, A. E. Finholt, J. R. Gilbrbath, H. R. Hoekstra and E. K. Hyde, *J. Am. Chem. Soc.*, 1953, **75**, 215–219; (b) E. Y. Marrero-Alfonso, A. M. Beaird, T. A. Davis and M. A. Matthews, *Ind. Eng. Chem. Res.*, 2009, **48**, 3703–3712; (c) Y. Zhu, L. Ouyang, H. Zhong, J. Liu, H. Wang, H. Shao, Z. Huang and M. Zhu, *Angew. Chem., Int. Ed.*, 2020, **59**, 8623–8629; (d) Y. Kojima, Y. Kawai, H. Nakanishi and S. Matsumoto, *J. Power Sources*, 2004, **135**, 36–41; (e) P. Brack, S. E. Dann and K. G. Upul Wijayantha, *Energy Sci. Eng.*, 2015, **3**, 174–188; (f) B. H. Liu and Z. P. Li, *J. Power Sources*, 2009, **187**, 527–534; (g) L. Ouyang, M. Liu, K. Chen, J. Liu, H. Wang, M. Zhu and V. Yartys, *J. Alloys Compd.*, 2022, **910**, 164831.
- (a) J. Y. Corey, *Adv. Organomet. Chem.*, 2004, **51**, 1–52; (b) E. M. Leitao, T. Jurca and I. Manners, *Nat. Chem.*, 2013, **5**, 817–829; (c) F. Gauvin, J. F. Harrod and H. G. Woo, *Adv. Organomet. Chem.*, 1988, **42**, 363–405; (d) T. D. Tilley, *Comments Inorg. Chem.*, 1990, **10**, 37–51; (e) T. D. Tilley, *Acc. Chem. Res.*, 1993, **26**, 22–29; (f) R. Waterman, *Chem. Soc. Rev.*, 2013, **42**, 5629–5641; (g) T. J. Clark, K. Lee and I. Manners, *Chem.–Eur. J.*, 2006, **12**, 8634–8648; (h) H. Yamashita and M. Tanaka, *Bull. Chem. Soc. Jpn.*, 1995, **68**, 403–419; (i) B. Marciniak, C. Pietraszuk, P. Pawluc and H. Maciejewski, *Chem. Rev.*, 2021, **122**, 3996–4090; (j) B. H. Kim, M. S. Cho and H. G. Woo, *Synlett*, 2004, 0761–0772.
- C. Aitken and J. F. Harrod, *J. Organomet. Chem.*, 1985, **279**, C11–C13.
- (a) J. F. Harrod, *Coord. Chem. Rev.*, 2000, **206–207**, 493–531; (b) J. Y. Corey, X. H. Zhu, T. C. Bedard and L. D. Lange, *Organometallics*, 1991, **10**, 924–930; (c) B. J. Grimmond and J. Y. Corey, *Organometallics*, 2000, **19**, 3776–3783; (d) A. D. Sadow and T. D. Tilley, *Organometallics*, 2003, **22**, 3577–3585.
- (a) I. Ojima, S. I. Inaba, T. Kogure and Y. Nagai, *J. Organomet. Chem.*, 1973, **55**, C7–C8; (b) L. Rosenberg, C. W. Davis and J. Yao, *J. Am. Chem. Soc.*, 2001, **123**, 5120–5121; (c) S. M. Jackson, D. M. Chisholm, J. S. McIndoe and L. Rosenberg, *Eur. J. Inorg. Chem.*, 2011, 327–330; (d) K. A. Brown-Wensley, *Organometallics*, 1987, **6**, 1590–1591; (e) L. S. Chang and J. Y. Corey, *Organometallics*, 1989, **8**, 1885–1893; (f) M. D. Fryzuk, L. Rosenberg and S. J. Rettig, *Inorg. Chim. Acta*, 1994, **222**, 345–364; (g) F. G. Fontaine, T. Kadkhodazadeh and D. Zargarian, *Chem. Commun.*, 1998, 1253–1254; (h) E. E. Smith, G. Du, P. E. Fanwick and M. M. Abu-Omar, *Organometallics*, 2010, **29**, 6527–6533; (i) F. G. Fontaine and D. Zargarian, *Organometallics*, 2002, **21**, 401–408; (j) B. P. Chauhan, T. Shimizu and M. Tanaka, *Chem. Lett.*, 1997, **26**, 785–786; (k) M. Tanabe, S. Iwase and K. Osakada, *Organometallics*, 2016, **35**, 2557–2562; (l) M. Tanabe, A. Takahashi, T. Fukuta and K. Osakada, *Organometallics*, 2013, **32**, 1037–1043.
- (a) B. Pribanic, M. Trincado, F. Eiler, M. Vogt, A. Comas-Vives and H. Grützmacher, *Angew. Chem. Int. Ed.*, 2020, **59**, 15603–15609; *Angew. Chem.*, 2020, **132**, 15733–15739; (b) S. I. Källäne, R. Laubenstein, T. Braun and M. Dietrich, *Eur. J. Inorg. Chem.*, 2016, 530–537; (c) D. Schmidt, T. Zell, T. Schaub and U. Radius, *Dalton Trans.*, 2014, **43**, 10816–10827; (d) J. Voigt, M. A. Chilleck and T. Braun, *Dalton Trans.*, 2013, **42**, 4052–4058.
- (a) N. P. Mankad, M. T. Whited and J. C. Peters, *Angew. Chem. Int. Ed.*, 2007, **46**, 5768–5771; *Angew. Chem.*, 2007, **119**, 5870–5873; (b) H. Schneider, D. Schmidt, A. Eichhöfer, M. Radius, F. Weigend and U. Radius, *Eur. J. Inorg. Chem.*, 2017, 2600–2616; (c) Y. Sunada, T. Imaoka and H. Nagashima, *Organometallics*, 2013, **32**, 2112–2120; (d) Y. Sunada, T. Imaoka and H. Nagashima, *Organometallics*, 2010, **29**, 6157–6160.
- (a) T. Tsumuraya, Y. Kabe and W. Ando, *J. Organomet. Chem.*, 1994, **482**, 131–138; (b) L. Roß and M. Dräger, *Z. Naturforsch.*



- B.*, 1983, **38**, 665–673; (c) W. P. Neumann and K. Kühlein, *Justus Liebigs Ann. Chem.*, 1965, **683**, 1–11.
- 10 (a) R. D. Miller and J. Michl, *Chem. Rev.*, 1989, **89**, 1359–1410; (b) R. G. Jones and S. J. Holder, *Polym. Int.*, 2006, **55**, 711–718; (c) R. West, *J. Organomet. Chem.*, 1986, **300**, 327–346.
- 11 C. Qing and C. Cui, *Dalton Trans.*, 2017, **46**, 8746–8750.
- 12 M. Okazaki, H. Kimura, T. Komuro, H. Okada and H. Tobita, *Chem. Lett.*, 2007, **36**, 990–991.
- 13 M. Itazaki, M. Kamitani, K. Ueda and H. Nakazawa, *Organometallics*, 2009, **28**, 3601–3603.
- 14 S. Pelzer, B. Neumann, H. G. Stämmler, N. Ignat'ev and B. Hoge, *Chem.–Eur. J.*, 2017, **23**, 12233–12242.
- 15 Y. Kobayashi and Y. Sunada, *Catalysts*, 2019, **10**, 29.
- 16 (a) E. Westhof and M. A. Sundaralingam, *J. Am. Chem. Soc.*, 1983, **105**, 970–976; (b) C. T. Altona and M. Sundaralingam, *J. Am. Chem. Soc.*, 1972, **94**, 8205–8212.
- 17 B. Jousseume, N. Noiret, M. Pereyre, A. Saux and J. M. Frances, *Organometallics*, 1994, **13**, 1034–1038.

